



Short communication

# COMETS2: An advanced MATLAB toolbox for the numerical analysis of electric fields generated by transcranial direct current stimulation

Chany Lee<sup>a</sup>, Young-Jin Jung<sup>b</sup>, Sang Jun Lee<sup>a</sup>, Chang-Hwan Im<sup>a,\*</sup><sup>a</sup> Department of Biomedical Engineering, Hanyang University, Seoul, Republic of Korea<sup>b</sup> Department of Radiological Science, Dongseo University, Busan, Republic of Korea

## HIGHLIGHTS

- We developed a MATLAB toolbox, COMETS2, for tDCS field analysis.
- COMETS2 can generate realistic rectangular pad electrodes at any scalp locations.
- A new technique for reducing computational time was proposed and implemented.
- COMETS2 is useful for repeatedly testing multiple electrode configurations and sizes.

## ARTICLE INFO

## Article history:

Received 1 October 2016

Received in revised form

12 December 2016

Accepted 13 December 2016

Available online 16 December 2016

## Keywords:

Neuromodulation

Transcranial direct current stimulation

(tDCS)

Finite element method (FEM)

Electrostatic field

MATLAB toolbox

## ABSTRACT

**Background:** Since there is no way to measure electric current generated by transcranial direct current stimulation (tDCS) inside the human head through in vivo experiments, numerical analysis based on the finite element method has been widely used to estimate the electric field inside the head. In 2013, we released a MATLAB toolbox named COMETS, which has been used by a number of groups and has helped researchers to gain insight into the electric field distribution during stimulation. The aim of this study was to develop an advanced MATLAB toolbox, named COMETS2, for the numerical analysis of the electric field generated by tDCS.

**New method:** COMETS2 can generate any sizes of rectangular pad electrodes on any positions on the scalp surface. To reduce the large computational burden when repeatedly testing multiple electrode locations and sizes, a new technique to decompose the global stiffness matrix was proposed.

**Results:** As examples of potential applications, we observed the effects of sizes and displacements of electrodes on the results of electric field analysis. The proposed mesh decomposition method significantly enhanced the overall computational efficiency.

**Comparison with existing methods:** We implemented an automatic electrode modeler for the first time, and proposed a new technique to enhance the computational efficiency.

**Conclusions:** In this paper, an efficient toolbox for tDCS analysis is introduced (freely available at <http://www.cometstool.com>). It is expected that COMETS2 will be a useful toolbox for researchers who want to benefit from the numerical analysis of electric fields generated by tDCS.

© 2016 Published by Elsevier B.V.

## 1. Introduction

Transcranial direct current stimulation (tDCS) is a noninvasive brain stimulation method that can modulate cortical excitability by transmitting small amounts of direct current (DC) between anode and cathode electrodes (Márquez-Ruiz et al., 2012; Nitsche et al.,

2008; Nitsche and Paulus, 2000). Although its underlying electrophysiological mechanisms have not yet been clearly revealed, tDCS has been applied to a variety of applications such as modulation of cognitive functions, neurorehabilitation, and potential treatment of brain diseases such as stroke, depression, Parkinson's disease, chronic pain, and epilepsy (Boggio et al., 2007; Coffman et al., 2012; Minamoto et al., 2014; Nelson et al., 2014; Nitsche et al., 2009). While it is known that the effect of tDCS is similar to that of repetitive transcranial magnetic stimulation (rTMS), tDCS has many advantages over rTMS such as better mobility and cost-effectiveness.

\* Corresponding author at: Department of Biomedical Engineering, Hanyang University, 222, Wangsimni-ro, Seongdong-gu, Seoul, 04763, Republic of Korea.  
E-mail address: [ich@hanyang.ac.kr](mailto:ich@hanyang.ac.kr) (C.-H. Im).

Currently, many researchers have realized that the estimation of stimulation current distribution inside the human head is important for successful brain stimulation with tDCS, because it was shown that the maximum current density is not always generated right below the stimulation electrodes. Recent studies have shown that the determination of electrode positions based on electric field analyses could significantly enhance the outcome of tDCS (Lee et al., 2015; Mendonca et al., 2011). Moreover, three-dimensional (3D) field simulations have elucidated the underlying mechanisms of volume current conduction (Rahman et al., 2013; Wagner et al., 2007), accelerated the development of new electrode montages (Ruffini et al., 2014), simulated special stimulation conditions (Datta et al., 2013; Parazzini et al., 2014), and decreased the necessity of massive experimental studies to verify the safety of tDCS (Im et al., 2012). In most of previous studies, the electric field distributions on the cortex were estimated using computer-based numerical analyses, since there is no way to directly measure the electric current inside the human head through in vivo experiments (Bikson et al., 2012).

Recently, some software tools for tDCS field simulation, such as SIMNIBS, BONSAI and SPHERES, have been introduced (Truong et al., 2014; Windhoff et al., 2013). SPHERES uses concentric spheres for the head model, which can provide intuitive understanding of the electric field distribution due to tDCS. BONSAI provides a web-based interface and thus can be easily accessed by its users although individual head models cannot be imported. In contrast, SIMNIBS enables the analyses of more complex head models based on the finite element method (FEM); however, it cannot automatically generate realistic tDCS electrodes on the scalp surface.

In 2013, our research team released a Windows-based graphical user interface (GUI) MATLAB toolbox named COMETS (COMputation of Electric field due to Transcranial current Stimulation), with the aim of providing unexperienced users with an easy way to simulate an electric field distribution due to tDCS inside a standard head model, based on 3D finite element analysis (FEA) (Jung et al., 2013). For the last three years, this MATLAB-based toolbox has been used to estimate the cortical current distribution due to tDCS by several research groups (Grabner et al., 2015; Heimrath et al., 2014; Hussey et al., 2015). However, the electrode modeling in COMETS is not realistic because forced boundary conditions were directly applied to scalp nodes; thus, the electrodes could not be modeled as exact rectangles. Furthermore, the default head model was a simple three-compartment model consisting of scalp, skull, and cerebrospinal fluid (CSF), and the brain area was not modeled separately, in order to reduce the overall computational burden.

In this paper, we introduce an advanced version of COMETS, named COMETS2, which is also a Windows-based MATLAB toolbox. In contrast to the previous version of COMETS, COMETS2 can automatically generate hexahedral electrode pads, simulating sponge-type electrodes, of which the sizes and angles are freely adjustable. A realistic human head model composed of scalp, skull, CSF, and brain (including both white matter and grey matter) is included as a default head model. User-generated head models can also be imported for individualized electric field simulations. Most importantly, an efficient technique for reducing the overall computational cost during the repeated field simulations is proposed. The detailed descriptions and examples of COMETS2 are provided in the following sections.

## 2. Methods

To estimate the electric potential and electric field intensity inside the human head, COMETS2 adopted FEM; however, since mesh generation of the head model is not supported in COMETS2, external mesh generation software needs to be used. We used

ISO2MESH software (Fang and Boas, 2009), a freely downloadable 3D mesh generator, to generate tetrahedral meshes from surface meshes. The surface meshes for four layers (scalp, outer skull boundary, inner skull boundary, and cortical surface) were generated from structural magnetic resonance imaging (MRI) data using CURRY7 for Windows (Compumedics NeuroScan, Charlotte, NC, USA). Other mesh generators such as SIMNIBS and BrainSuite can also be used for the generation of individual head surface meshes. A default head model included in COMETS2 was composed of 129,103 nodes and 804,251 elements. Note that the previous version of COMETS did not differentiate between the CSF and brain areas in order to reduce the overall computational time. In contrast, the current version of COMETS2 differentiates between those two areas thanks to the introduction of a new technique to accelerate computational time. The procedures of COMETS2 can be roughly divided into preprocessing and main processing steps. In the preprocessing step, the binary conversion of mesh data, surface extraction, mesh structure analysis, and construction of a system matrix for the initial mesh are performed. Users do not need to execute this preprocessing procedure more than once unless the head model is changed. The main processing step consists of automatic generation of electrodes and FEA. The GUI of the toolbox was optimized for the latest version of MATLAB (ver. R2015b) (MathWorks, Natick, MA, USA). Codes for binary conversion, surface extraction, mesh structure analysis, and FEA were written in FORTRAN90 and compiled using the Intel Fortran Compiler 10.0 (Intel, Santa Clara, CA, USA). We tested COMETS2 in 64-bit Windows 7 and Windows 10 environments installed in Intel i5 and i7 personal computer systems.

### 2.1. Preprocessing 1–binary conversion of mesh data

In COMETS2, NODE and ELE file formats of TETGEN (Si, 2015), a free tetrahedral mesh generator embedded in ISO2MESH (Fang and Boas, 2009), are read and saved as binary files, which are then used for the entire functions and subroutines of COMETS2. Conversion to a binary file format has several advantages over the use of ASCII (American standard code for information interchange) format in that it requires less storage space, takes less time for reading and writing, and shows a higher precision for floating-point numbers.

### 2.2. Preprocessing 2–surface extraction

The scalp surface and the cortical surface (i.e., the interface between the CSF and cortex) are extracted from the element data. In the default finite element data, the scalp surface contains 4936 nodes and 9868 triangles, and the cortical surface contains 35,057 nodes and 70,266 triangles. The extracted scalp mesh data are used for the generation of sponge electrodes. The cortical surface is used to visualize the resultant electric field distribution obtained from FEA.

### 2.3. Preprocessing 3–mesh structure analysis

One of the characteristics of FEM is the sparsity of the system matrix or global stiffness matrix (Jin, 2014), which means that most of the matrix elements are zeros. For example, if an  $i$ -th node is directly connected with  $N$  neighboring nodes, the  $i$ -th row of the global stiffness matrix has only  $N + 1$  nonzero entries. Furthermore, considering the symmetry of the stiffness matrix, the number of meaningful nonzero entries is very small compared to the number of all matrix elements. This sparse characteristic is generally taken into account in constructing a global stiffness matrix and in solving the linear matrix equation. In general, analyzing the mesh structure and finding the positions of nonzero entries is time consuming. Therefore, when a head model is fixed and the FEA needs

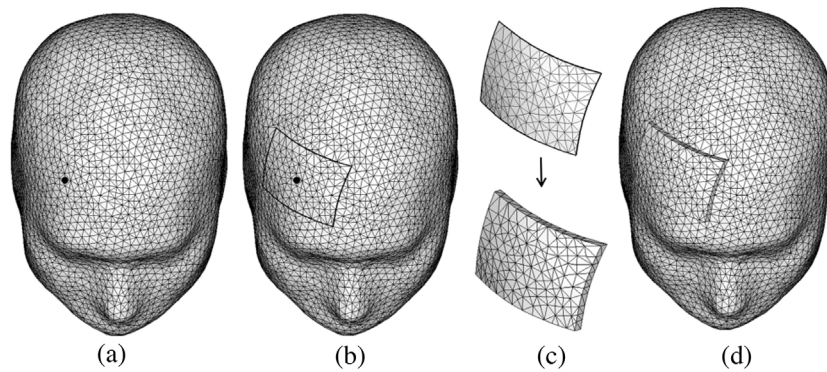


**Fig. 1.** An example of electrode generation. (a) Selection of center node. (b) Alignment of scalp nodes around the edges of the electrode. (c) Electrode generation. (d) Merging the electrode mesh into the initial mesh. After this process, the structure of the initial mesh is minimally modified.

to be repeatedly applied to the model, storing the results of the mesh structure analysis (positions of nonzero entries) can enhance the overall efficiency of the analyses, because these results are not changed unless the head model is changed.

#### 2.4. Preprocessing 4–construction of global stiffness matrix for initial mesh

A global stiffness matrix for an initial mesh (without electrodes in the model) was constructed prior to the automatic electrode generation. The governing equation used for the electric field analysis is an electrostatic Laplace's equation defined as

$$\nabla \cdot (\sigma \nabla V) = 0, \quad (1)$$

where  $\sigma$  and  $V$  are electrical conductivity and electric potential, respectively (Im et al., 2012). To consider the sparsity of the system matrix, we used a direct sparse solver (DSS) of the math kernel library (MKL) provided by Intel to solve the global matrix equation of FEM.

#### 2.5. Main processing 1–generation of electrode mesh

After a user selects the center position of an electrode (Fig. 1a), the scalp nodes around the edges of the electrode are moved and aligned so as to be fitted to the designated size and shape of the electrode, as shown in Fig. 1b. During this node alignment process, no additional scalp node needs to be generated. Using the aligned nodes, a mesh for the hexahedral electrode is independently generated using TETGEN (Si, 2015) included in the toolbox (Fig. 1c), and then merged into the initial mesh data (Fig. 1(d)). The generated electrode has a default thickness of 5 mm, and its conductivity can be easily set by the user.

#### 2.6. Main processing 2–finite element analysis

After the generation of meshes for two sponge electrodes, the global stiffness matrix needs to be updated to reflect the newly merged meshes. Since the global stiffness matrix for the initial mesh without electrodes was already constructed, the calculation of the element stiffness matrices is needed only for the elements that are newly generated inside the sponge electrodes and for the elements including nodes that have been moved and aligned to form the rectangular shapes of the electrode bottoms. Less than 200 nodes and 1000 elements were newly generated for a  $5 \times 7$  cm electrode, which is much smaller than the total number of nodes and elements of the head model. The input variables of DSS were updated only for the newly generated or modified element data, which considerably reduced the overall computational burden, compared to when

the whole stiffness matrix is recalculated. A schematic diagram for elucidating the strategy for updating the global stiffness matrix is illustrated in Fig. 2.

Dirichlet boundary conditions were applied on the upper sides of two sponge electrodes. Next, the electric current passing through the bottom of each electrode was calculated. Based on the linear relationship between the total injection current and the electromagnetic quantities of each node, the electric potential, electric field, and current density values in the entire analysis domain were scaled by the ratio of the user-defined target injection current to the computed injection current passing through the bottom of the electrode. The users can visualize the distributions of various physical quantities on the cortical surface, and probe the exact values at any user-selected points simply by clicking the mouse button.

### 3. Results

As application examples of COMETS2, we first tested the influence of electrode sizes on the resultant electric field distribution. The anode and cathode were attached to the right supraorbital area and FC3, respectively, according to the international 10-10

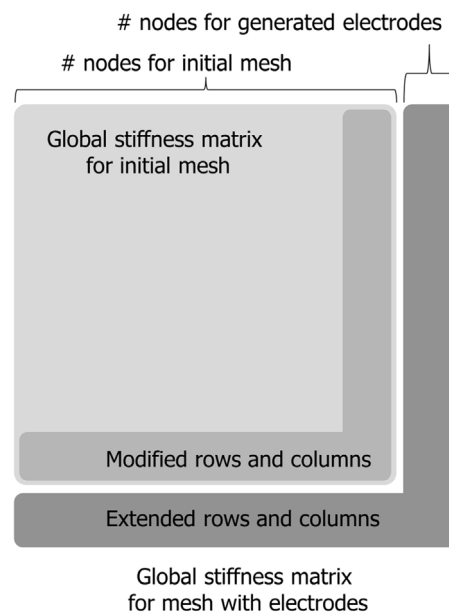


**Fig. 2.** Schematic diagram of the global stiffness matrix after electrode generation. The numbers of modified and added rows are small compared to the rank of the global stiffness matrix. Hence, the construction of the global stiffness matrix after electrode generation does not take much time.

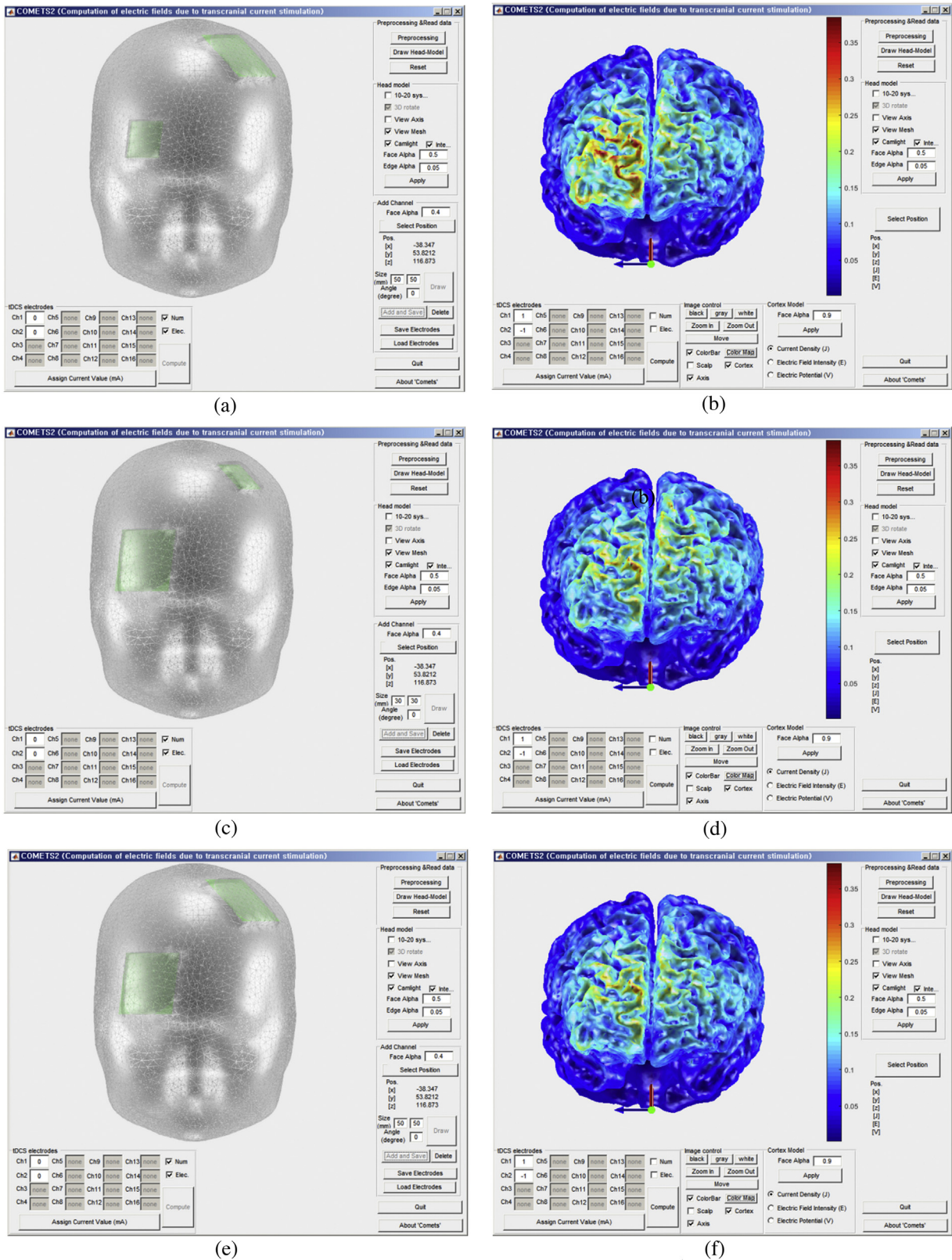


**Fig. 3.** Simulation results of three different combinations of 3 cm × 3 cm electrodes and 5 cm × 5 cm electrodes. Injected current was 1 mA for all cases. The scale of the color bar was adjusted to the same limits. (a) Anode: 3 cm × 3 cm, cathode: 5 cm × 5 cm. (b) Results of (a). (c) Anode: 5 cm × 5 cm, cathode: 3 cm × 3 cm. (d) Results of (c). (e) Anode: 5 cm × 5 cm, cathode: 5 cm × 5 cm. (f) Results of (e).

electrode placement system. As shown in Fig. 3, three models with different combinations of 3 × 3 cm electrodes and 5 × 5 cm electrodes were simulated. In these simulations, we assumed 1-mA

current injection. As a result, more focalized current density distributions were observed in the right prefrontal cortex when smaller

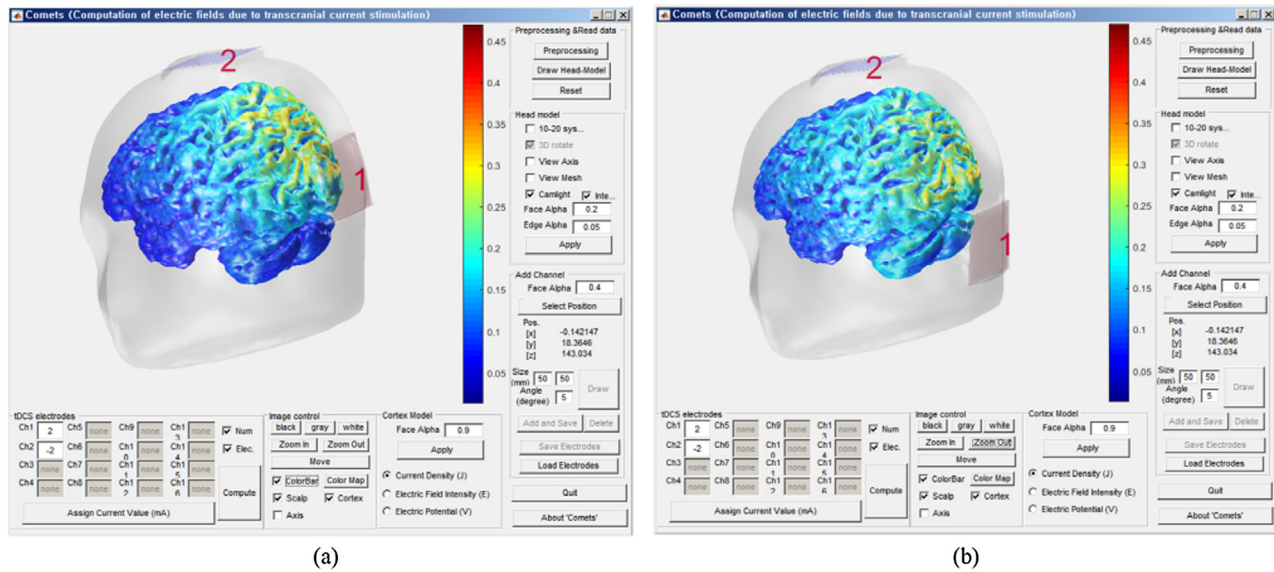


**Fig. 4.** Optimization of electrode position for stimulation of the visual cortex. (a) Conventional montage. (b) Optimized montage. More current could flow through the visual cortex with the optimized montage.

electrodes were used (see Fig. 3b). The size of the cathode did not significantly affect the resultant current density distribution.

Another application example of COMETS2 is given in Fig. 4, where the positions of the active electrode were optimized. In the previous literatures, active and reference electrodes were generally placed on Oz and Cz, respectively, to modulate the primary visual cortex (V1) (Antal et al., 2004; Spiegel et al., 2012). We first placed anode and cathode electrodes on Oz and Cz, respectively, to simulate the conventional electrode configuration. As seen in Fig. 4a, our simulation results demonstrated that the conventional Oz–Cz montage could not effectively stimulate V1, even though the anode was located right above V1. The electric field generated by the Oz–Cz montage was widely distributed not only on the occipital area, but also on the parietal area. To find a better montage for the optimal stimulation of V1, we gradually moved the anode along the midline. As a result, as shown in Fig. 4b, we found that placing the anode on an area approximately 4 cm inferior to Oz could best stimulate the visual cortex.

To validate the enhancement of computational efficiency of COMETS2 by adopting the new automatic electrode modeler and the new efficient technique for stiffness matrix construction, we compared the elapsed time between our method and the conventional approach that regenerated the entire head mesh after remodeling electrodes. A personal computer system with Intel i5-4670, 16G RAM, Windows 7 and MATLAB 2015b environments was used for the comparison study. It took 47.63 s to regenerate the 3D finite element model from surface mesh data with two  $5 \times 7$  cm electrodes using ISO2MESH, whereas it took just 5.72 s to separately generate mesh data for two  $5 \times 7$  cm sponge electrodes using TETGEN and merge them into the initial mesh data. Moreover, it took 9.55 s to construct the global stiffness matrix with the entirely regenerated head mesh data, while it took just 0.43 s to construct the global stiffness matrix with the partially regenerated mesh data. These results suggest that COMETS2 might be specifically useful for studies that involve repetitive analyses, e.g., finding optimal electrode positions to maximize the electric field at target brain areas, which requires repetitive simulations to test various electrode configurations.

An individual head model was also tested. As shown in Fig. 5a, a four-compartment head model composed of 140,496 nodes and 871,004 elements was generated from MRI data using SIMNIBS, ITK

(Yoo et al., 2002), and ISO2MESH. Fig. 5b shows an example of the electric field analysis using the individual head model.

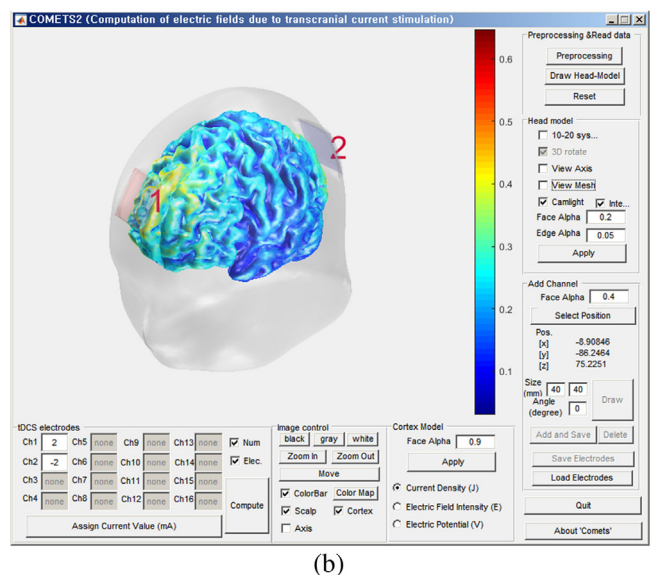
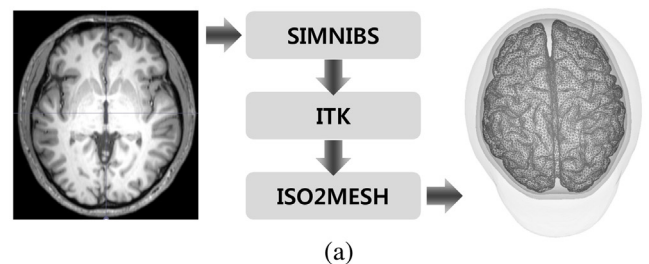


**Fig. 5.** Simulation of electric field with an individual head model: (a) generation of a four-compartment head model composed of 140,496 nodes and 871,004 elements, (b) an example of electric field analysis using the generated individual head model.

#### 4. Discussion

In this work, we developed a freely downloadable MATLAB toolbox, named COMETS2, for the analysis of the electric fields generated by tDCS. With the standard brain model included in COMETS2, any novice MATLAB user can simulate different electrode configurations with a variety of sizes and directions, from which they can gain insight into how the electric field under the scalp is formed and where the optimal electrode positions are to more effectively modulate the target brain regions of interest. Advanced users can import their own head models extracted from individual head MRI data, to which they can apply COMETS2 for the planning of individualized, image-guided neuromodulation. Compared to the previous version, COMETS2 was improved in many aspects. For example, a four-layer head model with a refined cortical surface model was used as a default model, and COMETS2 allows users to import their own head data. A detailed process to import five-layer head models generated using SIMNIBS is well documented in the user manual of COMETS2. Most importantly, the computational efficiency of COMETS2 was considerably improved. For instance, DSS of MKL was adopted to effectively solve the FEM, and some subroutines were programmed using OpenMP so that time-consuming iterations can be calculated using parallel processors (Dagum and Menon, 1998).

COMETS2 can automatically generate rectangular sponge-pad electrodes at any user-selected positions without a change in the overall mesh structures, which is one of the unique features of this toolbox. In many tDCS studies, electric current is applied using saline-soaked sponge electrodes (Fecteau et al., 2014; Fujimoto et al., 2014; Koo et al., 2015; Nelson et al., 2014; Tecchio et al., 2013). There are two approaches to handling the tDCS electrodes in the computer-based numerical analyses. One method, which was used in the previous version of COMETS2, is to apply Dirichlet boundary conditions on scalp nodes without the actual generation of sponge electrodes (Jung et al., 2013). This method is simple, but not at all realistic because a metal plate is usually placed only on the upper side of a sponge; thus, the interface between the scalp and the sponge is not equipotential. The other method is to generate a head model including sponge electrode pads and to apply boundary conditions only on the upper side of the sponge (Kessler et al., 2013). The latter is obviously more realistic than the former; however, every time the locations and sizes of the electrodes are changed, the finite element head model needs to be regenerated manually, and the global stiffness matrix needs to be constructed again, which takes considerable time and effort. In this study, instead of remodeling and regenerating the entire head model, we generated the electrode mesh separately and merged it with the original head mesh with only slight modifications in some node positions of the initial head mesh. This automatic process made only a small portion of the global stiffness matrix to be changed, which could reduce the overall computational time, as our comparison study demonstrated.

COMETS2 still has some limitations. First, our toolbox does not include any functionality for the segmentation or tessellation of structural MRI data; thus, only formatted data files can be imported. Hence, advanced users need to generate their own head models using other tools such as FREESURFER, FSL, SIMNIBS, or TETGEN (Fischl, 2012; Grabner et al., 2015; Jenkinson et al., 2012; Windhoff et al., 2013). The detailed descriptions on how to import the user's own data are provided in our user manual. Advanced users can also use separate 3D visualization program such as TEC-PLOT ([www.tecplot.com](http://www.tecplot.com)) or Mesh Viewer ([mview.sourceforge.net](http://mview.sourceforge.net)) using a resultant ASCII-format output file with an extension of \*.tec. Second, COMETS2 can be operated only under a Windows environment because some subroutines were built as Windows executable files. Third, COMETS2 does not consider the anisotropic

conductivity of the skull or the white matter, which requires additional computational burdens. Considering that the main advantage of the current version of the COMETS2 toolbox is the fast repetitive simulations of various electrode montages and sizes, we are not currently considering the inclusion of such functions in the COMETS2 toolbox. However, we are planning to develop another toolbox that can consider anisotropic conductivity. Our software toolbox will be updated seamlessly to include new functions such as automatic determination of electrode locations to deliver maximal current to a target area.

In this paper, a toolbox for the fast and realistic simulation of electric fields due to tDCS was introduced. COMETS2 can be downloaded from a website of the Computational Neuroengineering Laboratory in Hanyang University (<http://cone.hanyang.ac.kr>) or from <http://www.COMETS2tool.com>. Any constructive comments and questions are always welcomed through an official e-mail ([cometstool@gmail.com](mailto:cometstool@gmail.com)).

#### Acknowledgements

This research was supported by the Original Technology Research Program for Brain Science through the National Research Foundation of Korea (NRF) funded by the Ministry of Education, Science, and Technology (NRF-2015M3C7A1031969).

#### References

- Antal, A., Kincses, T.Z., Nitsche, M.A., Bartfai, O., Paulus, W., 2004. Excitability changes induced in the human primary visual cortex by transcranial direct current stimulation: direct electrophysiological evidence. *Investig. Ophthalmol. Vis. Sci.* 45, 702, <http://dx.doi.org/10.1167/iovs.03-0688>.
- Bikson, M., Rahman, A., Datta, A., 2012. Computational models of transcranial direct current stimulation. *Clin. EEG Neurosci.* 43, 176–183, <http://dx.doi.org/10.1177/1550059412445138>.
- Boggio, P.S., Nunes, A., Rigonatti, S.P., Nitsche, M.A., Pascual-Leone, A., Fregni, F., 2007. Repeated sessions of noninvasive brain DC stimulation is associated with motor function improvement in stroke patients. *Restor. Neurol. Neurosci.* 25, 123–129.
- Coffman, B.A., Trumbo, M.C., Clark, V.P., 2012. Enhancement of object detection with transcranial direct current stimulation is associated with increased attention. *BMC Neurosci.* 13, 108, <http://dx.doi.org/10.1186/1471-2202-13-108>.
- Dagum, L., Menon, R., 1998. OpenMP: an industry standard API for shared-memory programming. *IEEE Comput. Sci. Eng.* 5, 46–55, <http://dx.doi.org/10.1109/99.660313>.
- Datta, A., Dmochowski, J.P., Guleyupoglu, B., Bikson, M., Fregni, F., 2013. Cranial electrotherapy stimulation and transcranial pulsed current stimulation: a computer based high-resolution modeling study. *Neuroimage* 65, 280–287, <http://dx.doi.org/10.1016/j.neuroimage.2012.09.062>.
- Fang, Q., Boas, D.A., 2009. Tetrahedral mesh generation from volumetric binary and grayscale images. *Proc. - 2009 IEEE Int. Symp. Biomed. Imaging From Nano to Macro, ISBI 2009* 1142–1145. [10.1109/ISBI.2009.5193259](http://dx.doi.org/10.1109/ISBI.2009.5193259).
- Fecteau, S., Agosta, S., Hone-Blanchet, A., Fregni, F., Boggio, P., Ciraulo, D., Pascual-Leone, A., 2014. Modulation of smoking and decision-making behaviors with transcranial direct current stimulation in tobacco smokers: a preliminary study. *Drug Alcohol Depend.* 140, 78–84, <http://dx.doi.org/10.1016/j.drugalcdep.2014.03.036>.
- Fischl, B., 2012. FreeSurfer. *Neuroimage* 62, 774–781, <http://dx.doi.org/10.1016/j.neuroimage.2012.01.021>.
- Fujimoto, S., Yamaguchi, T., Otaka, Y., Kondo, K., Tanaka, S., 2014. Dual-hemisphere transcranial direct current stimulation improves performance in a tactile spatial discrimination task. *Clin. Neurophysiol.* 125, 1669–1674, <http://dx.doi.org/10.1016/j.clinph.2013.12.100>.
- Grabner, R.H., Rüttsche, B., Ruff, C.C., Hauser, T.U., 2015. Transcranial direct current stimulation of the posterior parietal cortex modulates arithmetic learning. *Eur. J. Neurosci.* 42, 1667–1674, <http://dx.doi.org/10.1111/ejn.12947>.
- Heimrath, K., Kuehne, M., Heinze, H.J., Zaehle, T., 2014. Transcranial direct current stimulation (tDCS) traces the predominance of the left auditory cortex for processing of rapidly changing acoustic information. *Neuroscience* 261, 68–73, <http://dx.doi.org/10.1016/j.neuroscience.2013.12.031>.
- Hussey, E.K., Ward, N., Christianson, K., Kramer, A.F., 2015. Language and memory improvements following tDCS of left lateral prefrontal cortex. *PLoS One* 10, 1–31, <http://dx.doi.org/10.1371/journal.pone.0141417>.
- Im, C.-H., Park, J.-H., Shim, M., Chang, W.H., Kim, Y.-H., 2012. Evaluation of local electric fields generated by transcranial direct current stimulation with an extracranial reference electrode based on realistic 3D body modeling. *Phys. Med. Biol.* 57, 2137–2150, <http://dx.doi.org/10.1088/0031-9155/57/8/2137>.

- Jenkinson, M., Beckmann, C.F., Behrens, T.E.J., Woolrich, M.W., Smith, S.M., 2012. *Fsl. Neuroimage* 62, 782–790, <http://dx.doi.org/10.1016/j.neuroimage.2011.09.015>.
- Jin, J., 2014. *The Finite Element Method in Electromagnetics, 3rd ed. Media. Wiley, New Jersey*.
- Jung, Y.-J., Kim, J.-H., Im, C.-H., 2013. COMETS: A MATLAB toolbox for simulating local electric fields generated by transcranial direct current stimulation (tDCS). *Biomed. Eng. Lett.* 3, 39–46, <http://dx.doi.org/10.1007/s13534-013-0087-x>.
- Kessler, S.K., Minhas, P., Woods, A.J., Rosen, A., Gorman, C., Bikson, M., 2013. Dosage considerations for transcranial direct current stimulation in children: a computational modeling study. *PLoS One* 8, e76112, <http://dx.doi.org/10.1371/journal.pone.0076112>.
- Koo, Y.S., Kim, S.M., Lee, C., Lee, B.U., Moon, Y.J., Cho, Y.W., Im, C.-H., Choi, J.W., Kim, K.H., Jung, K.-Y., 2015. Transcranial direct current stimulation on primary sensorimotor area has no effect in patients with drug-naïve restless legs syndrome: a proof-of-concept clinical trial. *Sleep Med.* 16, 280–287, <http://dx.doi.org/10.1016/j.sleep.2014.07.032>.
- Lee, M., Kim, Y.-H., Im, C.-H., Kim, J.-H., Park, C., Chang, W.-H., Lee, A., 2015. What is the optimal anodal electrode position for inducing corticomotor excitability changes in transcranial direct current stimulation? *Neurosci. Lett.* 584, 347–350, <http://dx.doi.org/10.1016/j.neulet.2014.10.052>.
- Márquez-Ruiz, J., Leal-Campanario, R., Sánchez-Campusano, R., Molae-Ardekani, B., Wendling, F., Miranda, P.C., Ruffini, G., Gruart, A., Delgado-García, J.M., 2012. Transcranial direct-current stimulation modulates synaptic mechanisms involved in associative learning in behaving rabbits. *Proc. Natl. Acad. Sci. U. S. A.* 109, 6710–6715, <http://dx.doi.org/10.1073/pnas.1121147109>.
- Mendonça, M.E., Santana, M.B., Baptista, A.F., Datta, A., Bikson, M., Fregni, F., Araujo, C.P., 2011. Transcranial DC stimulation in fibromyalgia: optimized cortical target supported by high-resolution computational models. *J. Pain* 12, 610–617, <http://dx.doi.org/10.1016/j.jpain.2010.12.015>.
- Minamoto, T., Azuma, M., Yaoi, K., Ashizuka, A., Mima, T., Osaka, M., Fukuyama, H., Osaka, N., 2014. The anodal tDCS over the left posterior parietal cortex enhances attention toward a focus word in a sentence. *Front. Hum. Neurosci.* 8, 992, <http://dx.doi.org/10.3389/fnhum.2014.00992>.
- Nelson, J.T., McKinley, R.A., Golob, E.J., Warm, J.S., Parasuraman, R., 2014. Enhancing vigilance in operators with prefrontal cortex transcranial direct current stimulation (tDCS). *Neuroimage* 85, 909–917, <http://dx.doi.org/10.1016/j.neuroimage.2012.11.061>.
- Nitsche, M.A., Paulus, W., 2000. Excitability changes induced in the human motor cortex by weak transcranial direct current stimulation. *J. Physiol.* 527 (Pt. 3), 633–639, <http://dx.doi.org/10.1111/j.1469-7793.2000.t01-1-00633.x>.
- Nitsche, M.A., Cohen, L.G., Wassermann, E.M., Priori, A., Lang, N., Antal, A., Paulus, W., Hummel, F., Boggio, P.S., Fregni, F., Pascual-Leone, A., 2008. Transcranial direct current stimulation: state of the art 2008. *Brain Stimul.* 1, 206–223, <http://dx.doi.org/10.1016/j.brs.2008.06.004>.
- Nitsche, M.A., Boggio, P.S., Fregni, F., Pascual-Leone, A., 2009. Treatment of depression with transcranial direct current stimulation (tDCS): a review. *Exp. Neurol.* 219, 14–19, <http://dx.doi.org/10.1016/j.expneurol.2009.03.038>.
- Parazzini, M., Focchi, S., Liorni, I., Priori, A., Ravazzani, P., 2014. Computational modeling of transcranial direct current stimulation in the child brain: implications for the treatment of refractory childhood focal epilepsy. *Int. J. Neural Syst.* 24, 1430006, <http://dx.doi.org/10.1142/S012906571430006X>.
- Rahman, A., Reato, D., Arlotti, M., Gasca, F., Datta, A., Parra, L.C., Bikson, M., 2013. Cellular effects of acute direct current stimulation: somatic and synaptic terminal effects. *J. Physiol.* 591, 2563–2578.
- Ruffini, G., Fox, M.D., Ripolles, O., Miranda, P.C., Pascual-Leone, A., 2014. Optimization of multifocal transcranial current stimulation for weighted cortical pattern targeting from realistic modeling of electric fields. *Neuroimage* 89, 216–225.
- Si, H., 2015. TetGen, a delaunay-based quality tetrahedral mesh generator. *ACM Trans. Math. Softw.* 41, 1–36, <http://dx.doi.org/10.1145/2629697>.
- Spiegel, D.P., Hansen, B.C., Byblow, W.D., Thompson, B., 2012. Anodal transcranial direct current stimulation reduces psychophysically measured surround suppression in the human visual cortex. *PLoS One* 7, 1–9, <http://dx.doi.org/10.1371/journal.pone.0036220>.
- Tecchio, F., Cancelli, A., Cottone, C., Tomasevic, L., Devigus, B., Zito, G., Ercolani, M., Carducci, F., 2013. Regional personalized electrodes to select transcranial current stimulation target. *Front. Hum. Neurosci.* 7, 131, <http://dx.doi.org/10.3389/fnhum.2013.00131>.
- Truong, D.Q., Hüber, M., Xie, X., Datta, A., Rahman, A., Parra, L.C., Dmochowski, J.P., Bikson, M., 2014. Clinician accessible tools for GUI computational models of transcranial electrical stimulation: BONSAI and SPHERES. *Brain Stimul.* 7, 521–524, <http://dx.doi.org/10.1016/j.brs.2014.03.009>.
- Wagner, T., Fregni, F., Fecteau, S., Grodzinsky, A., Zahn, M., Pascual-Leone, A., 2007. Transcranial direct current stimulation: a computer-based human model study. *Neuroimage* 35, 1113–1124, <http://dx.doi.org/10.1016/j.neuroimage.2007.01.027>.
- Windhoff, M., Opitz, A., Thielscher, A., 2013. Electric field calculations in brain stimulation based on finite elements: an optimized processing pipeline for the generation and usage of accurate individual head models. *Hum. Brain Mapp.* 34, 923–935, <http://dx.doi.org/10.1002/hbm.21479>.
- Yoo, T.S., Ackerman, M.J., Lorensen, W.E., Schroeder, W., Chalana, V., Aylward, S., Metaxas, D., Whitaker, R., 2002. *Engineering and algorithm design for an image processing Api: a technical report on ITK-the Insight Toolkit. Stud. Health Technol. Inform.* 85, 586–592.